Original Article

Journal of Food Safety and Hygiene

Journal homepage: http://jfsh.tums.ac.ir

Molecular modeling of azo-food dye metabolites in the brain and their effects on attention deficit and hyperactivity disorder (ADHD) using ArgusLab software

Katyayani Verma[1], Rajendra Prasad[2,3]*

[1]*Wuhan University School of Medicine, Wuhan, Hubei Province, China.*
[2]*Rajendra Academy, Vivekanandapuram, Varanasi, India.*
[3]*Department of Chemistry, Fiji National University, Natabua Campus, Lautoka, Fiji.*

ARTICLE INFO

Article history:
Received 19.10. 2024
Received in revised form 18.12.2024
Accepted 23.12.2024

Keywords:
ADHD;
Attention deficit hyperactivity;
Azo dye;
Food color;
Metabolite;
Synthetic dye

ABSTRACT

This study hypothesizes that the attention deficit and hyperactivity disorder (ADHD) effect of azo food dyes could arise from their hydroxylated amine metabolites. These metabolites are generated either by the action of body's enzymes or by the intestinal microbiome. The blood-brain barrier (BBB) penetration and competitive binding abilities of metabolites with dopamine receptors in the brain are investigated. Geometries of metabolites were optimized using quantum chemical Austin Model 1 (AM1). Lipophilicity, diffusion coefficient, topological polar surface area, and hydrogen bonding atom distances were calculated for the metabolites in the optimized geometries. Based on BBB penetrability as well as the competitive binding abilities of metabolites with dopamine receptors, it is concluded that the metabolites of Amaranth dye are likely to cause the strongest ADHD effect, followed by Ponceau 4R and Allura Red. Dyes Sunset yellow, Azorubine and Tartrazine could cause milder ADHD effects in that order. Besides relative grading of water-soluble food dyes for their ADHD potential, the study provides an alternative model for molecular basis of origin of ADHD and provides plausible reasons for its differential manifestation in different children.

Citation: Verma K, Prasad R. **Molecular Modeling of azo-food dye metabolites in brain and their effects on attention deficit and hyperactivity disorder (ADHD) using ArgusLab software.** J Food Safe & Hyg 2024; 10 (4):270-283.http://doi.org/10.18502/jfsh.v10i4.19392

1. Introduction

Food colors are implicated in causing attention deficit hyperactivity disorder (ADHD) in children and young adults (1 - 4), which is the most commonly diagnosed mental disorder in this age group.

*Corresponding author. Tel.: +91 96213 05125
E-mail address: rajenfcy@gmail.com

ADHD is characterized by excess inattention, impulsivity and hyperactivity. The inattention is manifested in difficulty in focusing, organizing and staying on any task; hyperactivity manifests in excessive movement, restlessness, and difficulty in

sitting still. Impulsivity leads to acting without thinking, interrupting, and difficulty waiting for turns. The colorants used in foods and beverages are mostly the water-soluble dyes of synthetic or natural origin. Synthetic azo dyes are one main group of colorants that are added in foods and beverages, particularly in confectionery, ice cream, fruit juices, soft drinks, biscuits, pastry products, cakes and processed meats.

All of the six approved azo food dyes, viz. allura red, azorubine, sunset yellow, tartrazine, ponceu 4R and amaranth dyes raise health concerns of varying degrees. It is often argued that they have not been adequately tested for carcinogenicity, genotoxicity, and hypersensitivity effects (5, 6). Population exposure to food dyes need not be limited to permitted dyes only, as unauthorized uses lead to far serious exposure risks (7). Even the non-ionic, fat-soluble azo dyes, banned for food use, e.g. Sudan I, II, III, IV and Para Red dyes are often illegally used to maintain the color in food products due to bright staining power, low cost and easy availability (8).

ADHD normally afflicts children and young adults (3). The etiology of ADHD appears to be multifactorial and involves a variety of chemical and neuron-physiological factors (9). Among the chemical factors food dyes and additives are mainly implicated in the induction and severity of ADHD, besides the chronic deficiency of micronutrients such as zinc, iron, magnesium, iodine and polyunsaturated fatty acids (PUFA) (10).

Most of the studies on ADHD have reported worsening of children's behavior after consumption of synthetic food dyes and additives (11). Not all, but a significant proportion of children respond adversely upon exposure to synthetic food dyes and the proportion of children getting affected increases with increasing the challenge dose (12). Sensitive individuals also exhibited altered physiological responses in their electroencephalograms (EEG) upon exposure to certain foods (13). Given the potentially negative behavioral effects of food dyes, it is important to determine why only some children show adverse behavioral reactions (14).

Three types of potential mechanisms,, toxicological, antinutritional, and hypersensitivity, are thought to be operative (12, 14). It is widely believed that the underlying mechanism of the development of ADHD might be similar to hypersensitivity and allergy. However, the causal relationship between ADHD and allergies is conflicting. Azo food dyes have been in widespread use for over past five decades, but adverse allergic reactions are rather mild, mostly involving the skin, and rarely leading to anaphylaxis (11).

Metabolism of azo food dyes has been comprehensively reviewed by Walker (15). Azo dyes are reasonably well absorbed upon oral or parenteral administration. Water-soluble azo dyes often undergo reductive cleavage to corresponding amines (reaction 1), by the mammalian as well as by gut microbial reductase enzymes (15 - 18). Mammalian liver extract under anaerobic conditions causes reductive cleavage of azo groups. Lactic acid bacteria (LAB), *Enterococcus faecalis,* and *Escherichia coli,* etc. have been demonstrated to do so. The rate and extent of reductive cleavage are influenced by the reduction potential of the dye molecule and the partial pressure of oxygen (pO2). At lower pO2 in the intestine, microbial reductive cleavage is the dominant pathway. The amine derivatives thus formed are excreted in urine and to a lesser extent in feces (18). It is important to

note that intravenous or intraperitoneal administration of water-soluble azo dyes leads to their quantitative excretion in urine with very little or no reductive cleavage.

$NaO_3S\text{-}Ar^1\text{-}N{=}N\text{-}Ar^2\text{-}SO_3Na \rightarrow NaO_3S\text{-}Ar^1\text{-}NH_2 + NaSO_3\text{-}Ar^2\text{-}NH_2$ (1)

$NaO_3S\text{-}Ar^1\text{-}NH_2 \rightarrow HO\text{-}Ar^1\text{-}NH_2$ (2a)

$NaSO_3\text{-}Ar^2\text{-}NH_2 \rightarrow HO\text{-}Ar^2\text{-}NH_2$ (2b)

Hydroxylation in the aromatic ring is an important pathway that often accompanies the desulphonation in the metabolism of azo dye metabolites (reactions 2a and 2b). It has been shown that in cases where reductive cleavage leads to the formation of unsulphonated amines, hydroxylation is often a major metabolic pathway before excretion. For example, the Red 2G, Red 10B, Sudan I, Orange RN, and Orange G dyes that formed aniline as the primary metabolite, which gets excreted in the urine largely as *p*-aminophenol, free and conjugated with glucuronic acid. Smaller amounts of *o*-aminophenol are also formed, while <1% was excreted as unhydroxylated aniline (19). Dealkylation of alkyl amino groups and oxidation of the methyl groups to carboxylic acid were also observed in the metabolism of water-insoluble dyes (19). The metabolism of azo food dyes is summarized in Scheme 1.

The interface between blood and brain is mediated by densely packed endothelial cells in brain capillaries together with a covering of glial cells overlying them, called blood blood-brain barrier (BBB) (20). BBB allows for highly selective movement of molecules and drugs. On a molecular level, the BBB is not homogeneous, but consists of several partially overlapping zones contained in a highly anisotropic lipid bilayer (21). Transport across the BBB may involve passive diffusion, facilitated diffusion, or active transport. However, for the majority of drug molecules, BBB penetration occurs through passive diffusion through the cellular membrane. Molecules undergoing transcellular diffusion over the BBB can also get metabolized by the cellular enzymes during the process (22).

This present study aims investigate investigating ADHD effect of azo food dyes from a neuro-physiological perspective. It is hypothesized that ADHD effects could arise from interference in the mesolimbic and mesocortical reward pathways via dopamine (DA) receptors (23, 24). Azo dyes, being highly water soluble, it is not the dye *per se*, but the enzymatic and gut-microbe generated metabolites from azo dyes (16, 25), could penetrate through the blood-brain barrier (BBB) and thereby can act as a dopamine agonist or antagonist. The chemical nature of azo dye metabolites is determined from literature sources, and the physico-chemical properties for BBB penetration and DA receptor binding are investigated *in-silico* using molecular modeling software.

2. Materials and Methods

Molecular geometries and electrostatic potential calculations of metabolites were carried out using ArgusLab 4.0 software (26). It is a powerful tool in molecular modeling, graphics, structure visualization and drug design programs for Windows operating

systems. Developed by Mark Thompson and Planarial Software LLC, it is freely licensed. Software facilitates building 3D-structures of molecules and offers a wide selection of methods for optimization of their geometries, viz. Austin Model 1 (AM1), parametric method 3 (PM3), and Modified Neglect of Diatomic Overlap (MNDO) semi-empirical quantum mechanical methods, Universal Force Field (UFF) and Amber molecular mechanics methods, as well as Hartree-Fock self-consistent field method. This facilitates visualization of molecular orbitals, molecular surface, and colored visualization of electrostatic potential (i.e., partial charges) on different atoms. Also, it exports atomic coordinates in easily readable XYZ format.

Molecular geometries were optimized using the semi-empirical Universal Force Field method, while electrostatic potentials (ESP) were calculated using quantum chemical Austin Model 1 (AM1), which is based on the Neglect of Differential Diatomic Overlap (NDDO) integral approximation (27). Lipophilicity (clogP) and topological polar surface area (TPSA) of the metabolites were calculated using MedChem Designer 5.0 (28) and OSIRIS Property Explorer software (29) on optimized geometries of the molecules. The calculated values of clogP and TPSA for sulphonated metabolites are for the corresponding protonated acid analogue, –SO3H, which would be lower than that of the corresponding anionic –SO3- forms.

It is presumed that the intestinal environment is reasonably anaerobic and the microbial fauna resident there is capable of quantitative reductive dissociation as well as hydroxylation of azo dyes to a comparable extent.

3. Results

The chemical nature of food dyes vis-à-vis their breakdown products based on reported metabolic pathways for azo food dyes is shown in Scheme 1. QSAR characteristics of the azo food dye metabolites are summarized in Table 1, and selected data are graphically presented in Figures 2 – 4. The interatomic distances among donor atoms in dopamine (DA), selected azo dye metabolites, and DA agonists are listed in Table 2. A comparison is made with 3 known DA agonists, viz. 3-amino-6,7-dihydroxy-1,2,3,4-tetrahydronaphthalene (ADTN), 5,6,6a,7,8,12b-hexahydro-benzo(a)phenanthridine-10,11-diol (dihydrexidine), and 8-hydroxy-2-(N,N-di-*n*-propylamino)tetralin (8-OH-DPAT). As seen from the table, molecular weights, number of hydrogen bond donors and hydrogen bond atoms for all of the azo food dye metabolites are favorable for BBB penetration. Qualitative comparison of parameters is given in Table 3.

Softwares employ different algorithms in the calculation of lipid solubility in terms of n-octanol/water partition coefficient and rate of diffusion of species. The OSIRIS Property Explorer calculates log(octanol/c_{water}), i.e., clogP, accounting only neutral forms of molecules, while MedChem Designer calculates topological polar surface area (TPSA), Hayduk and Laudie's estimation of diffusion coefficients (DiffCoef), and n-octanol/water partition coefficient, accounting for ionized and non-ionized forms both as S+logP and S+logD, respectively, as well as MlogP using Moriguchi logP model.

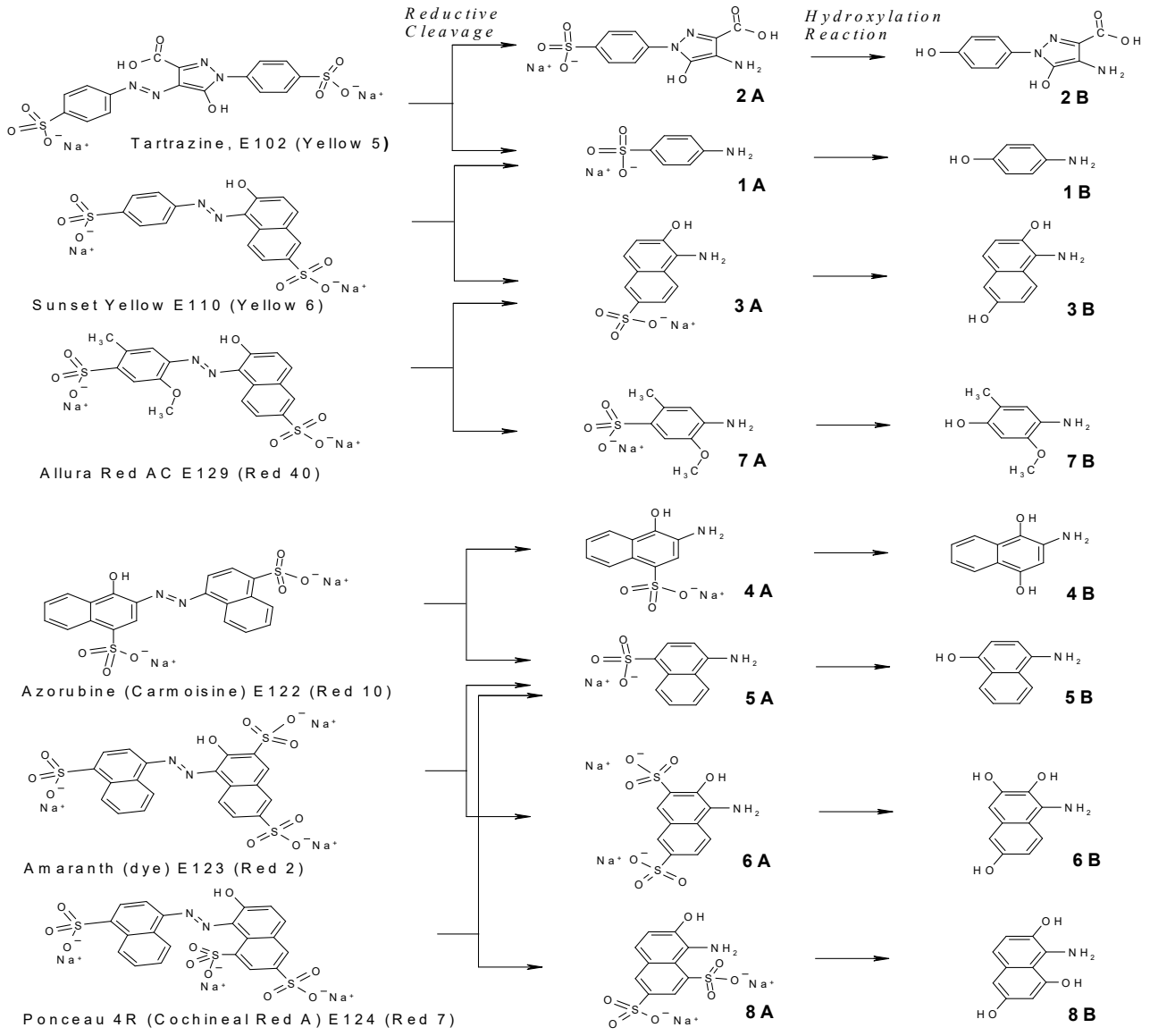

Figure 1. Molecular structure of azo food dyes and their metabolites

Table 1. Calculated QSAR parameters for azo dye metabolites and dopamine agonists

Molecule	Molecular Weight	clogP [a]	TPSA [b]	DiffCoef [c]	MlogP [d]	S+logP [e]	S+logD [f]	M_NO [g]	HBDH [h]
1A	173	-1.25	80	1.087	-0.115	-1.866	-1.649	4	3
1B	109	0.64	46	1.331	0.893	0.283	0.281	2	3
2A	299	-2.53	156	0.842	-0.574	-0.858	-2.015	9	5
2B	235	-0.65	122	0.953	0.258	0.93	-1.097	7	5
3A	239	-0.40	101	0.917	1.022	-0.853	-1.362	5	4
3B	175	1.49	66	1.061	1.967	1.535	1.533	3	4
4A	239	-0.40	101	0.917	1.022	-1.07	-2.049	5	4
4B	175	1.49	66	1.061	1.967	1.348	1.345	3	4
5A	223	-0.05	80	0.935	1.03	-0.966	-1.554	4	3
5B	159	1.83	46	1.087	2.024	1.621	1.62	2	3
6A	319	-2.63	155	0.804	-0.331	-1.773	-1.93	8	5
6B	155	1.14	76	1.144	0.65	0.135	0.131	4	4
7A	219	-0.35	110	0.972	-0.274	-1.591	-1.888	6	4
7B	153	0.91	55	1.087	1.5	0.86	0.855	3	3
8A	319	-2.63	155	0.804	-0.331	-2.229	-2.089	8	5
8B	191	1.14	87	1.037	1.428	1.327	1.311	4	5
ADTN	179	0.88	66	1.014	1.484	0.166	-1.333	3	4
Dihydrexidine	267	1.79	52	0.816	3.082	2.256	1.671	3	3
Dopamine	153	0.40	66	1.087	1.255	-0.313	-1.823	3	4
8-OH-DPAT	247	3.56	23	0.76	3.154	3.4	1.35	2	1

[a]: Calculated $\log(c_{octanol}/c_{water})$ for neutral species,
[b]: Topological Polar Surface Area,
[c]: Rate of diffusion m^2/s,
[d]: $\log(c_{octanol}/c_{water})$ calculation using Moriguchi model,
[e]: Specific $\log(c_{octanol}/c_{water})$ accounting ionized and non ionized forms both,
[f]: Specific rate of diffusion m^2/s accounting for ionized and non-ionized forms both
[g]: Number of N and O atoms
[h]: Number of OH and NH hydrogen bond donor Hydrogen atoms

4. Discussion

The numeric values of molecular weight, lipophilicity (clogP, S+logP, MlogP) and topological polar surface area (TPSA) of the dye metabolites are considered to be critical parameters for grading their entry into the brain.

The mean value ($\bar{x}$) of the reported range for each parameter is considered to be the most optimum, and ±1σ, ±2σ are incrementally assigned lower significance. For the sake of lipophilicity comparisons, clogP values are used in the discussion hereafter, as more literature data is available on its utility in determining BBB penetration ability of drugs and other molecules. Pajouhesh describes that size, ionizability, flexibility, and hydrogen bonding ability of molecules a critical role in determining their CNS uptake profile (22). Examination of QSAR descriptors of CNS drugs showed that lipophilicity (clogP ≤ 5; molecular weight ≤ 500; polar surface area of 60 – 70 $Å^2$ and hydrogen bonding atoms ≤ 10 plays a predominant role in BBB penetration (21,22,30). To a smaller extent, other characteristics like limited flexibility, i.e., 5 or fewer rotatable bonds, presence of tertiary nitrogen, and ability to acquire positive charge at pH 7-8 also aid in BBB penetration. Polar molecules are generally poor CNS agents unless they undergo active transport across the CNS.

As we know, the hydrophilic/lipophilic interface at the blood/cell-membrane boundary consists of perturbed and bound water and negatively charged polar lipid heads connected to long hydrophobic chains. Thus, any molecule approaching the BBB is confronted with a thick layer that is capable of non-covalent interactions with only a little steric requirement. The conformational mobility of the lipid chains is relatively low at the lipid head, i.e., near the blood/lipid interface, and increases strongly towards the center of the bilayer. As a result, the moderately lipophilic molecules easily cross the BBB through passive diffusion.

The diversity and population density of gut microbes vary from individual to individual depending upon their food habits, environmental conditions, and genetic disposition (31-33). It could be reasonably expected that the extent of formation of aryl amino phenols, the potential neuron transmitters, would vary in individuals for the same challenge dose of the azo dye.

4.1. Lipophilicity of azo dye metabolites

The lipophilicity is an important consideration for the penetration of blood-brain barrier. Calculated lipophilicity values are shown in **Fig. 2**. Analysis of small drug-like molecules shows that for efficient BBB penetration, LogP values should be greater than 1.5 and less than 2.7 (22). Whereas, for efficient intestinal absorption, logD values need to be in the range of 0 – 3 (22). All hydroxylated metabolites except 2B and drug dihydrexidine were found to exhibit favorable clogP and logD values. Considering the optimum range for BBB penetration, the penetrability order could be inferred as 5B > 7B > 3B = 4B > 6B = 8B > 1B. The metabolite 2B shows a negative clogP value, and even supposing it undergoes decarboxylation during transcellular diffusion resulting metabolite 2C still possesses an unfavorable negative clogP of -0.14. Among the agonists, ADTN had a comparable clogP to that of 7B, but DPAT had a much higher value and thereby is expected to penetrate poorly to the brain, by being retained in the lipid bilayer.

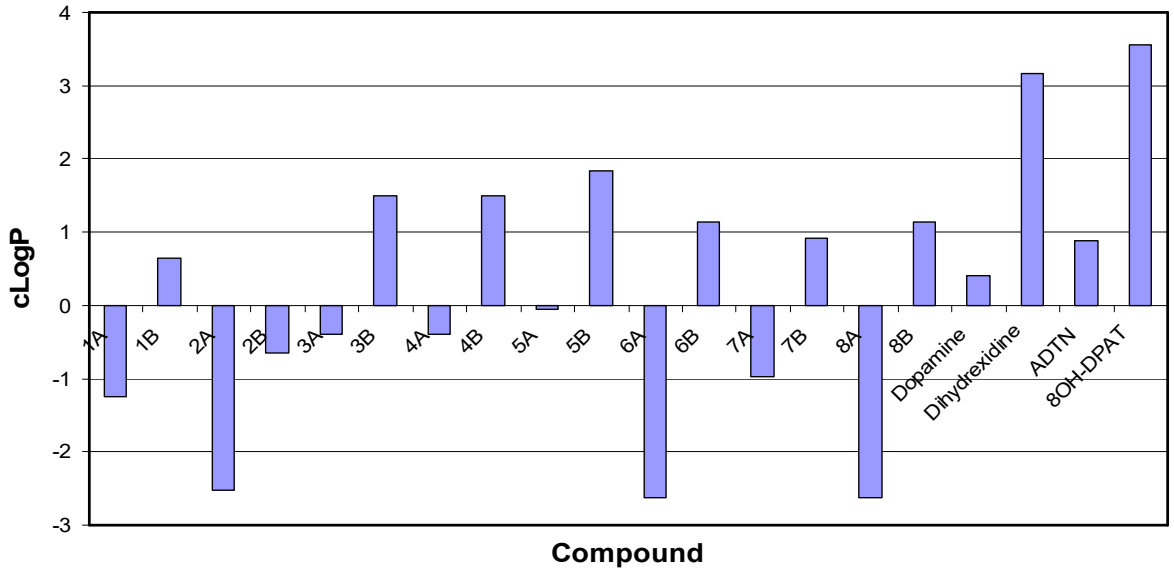

Figure 2. Plot of Lipophilicity of azo dye metabolites, dopamine and dopamine agonists

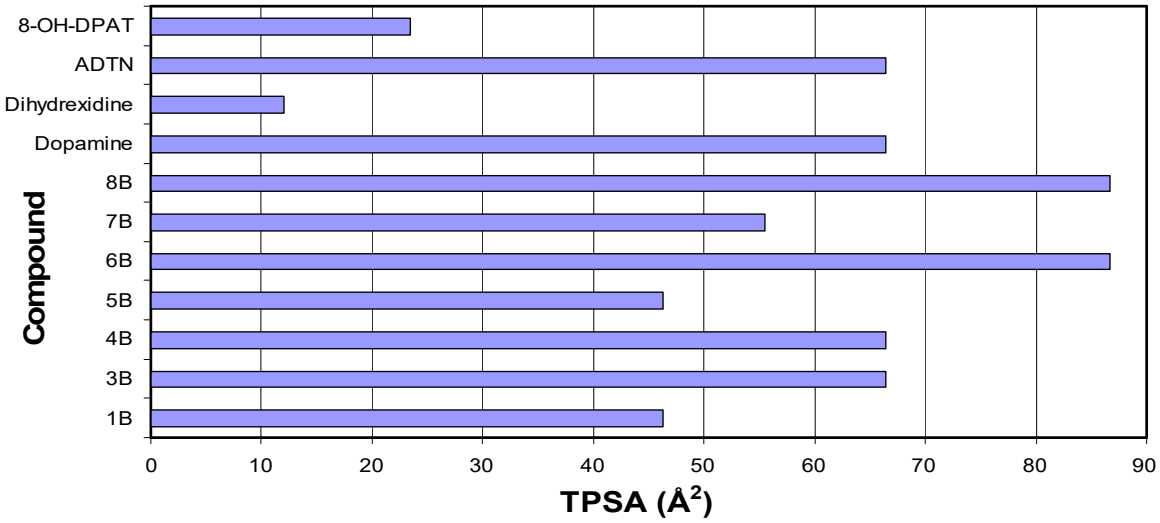

Figure 3. Plot of topological polar surface area (TPSA) of azo dye metabolites, dopamine, and dopamine agonists

http://doi.org/10.18502/jfsh.v10i4.19392/jfsh.v10i4.19392

4.2. TopologicalTopological polar surface area (TPSA) of azo dye metabolites

Calculated TPSA values of all metabolites are listed in Table 1, and of selected metabolites with favorable cLogP are shown in Fig. 3. Studies have demonstrated that compounds with TPSA values in the range of 60 – 70 $Å^2$ have exhibited efficient brain penetration, and the upper limit for TPSA for a molecule to penetrate the brain is around 90 $Å^2$ (21,22). Thus, metabolites 3B, 4B, 6B, and 7B, and to some extent 8B, meet this requirement. The 3B, 4B, and 7B showed the optimum TPSA for passive BBB penetration. The calculated TPSA value for ADTN was also in the optimum range, but that of dihydrexidine and DPAT was much lower.

4.3. Ligand binding ability of azo and dye metabolites

The electrostatic potential (ESP) maps of hydroxylated metabolites, 1B – 8B, are shown in **Fig. 4**. Structures show that they are all moderately polar, semi-rigid molecules having negative electrostatic potentials over N and O atoms. The hetero atoms in these metabolites are capable of exerting dipolar and hydrogen bonding interactions with the dopamine receptor proteins (22,30). Interatomic distances between these hetero atoms play a key role in potential ligand binding interactions at a DA receptor center. The calculated O, O, O and N, O, O distances in hydroxylated metabolites, dopamine, and dopamine agonists are listed in Table 2. Closer correspondence in all three distances in a metabolite vis-à-vis dopamine could lead to competitive interaction with the DA-receptor, whereas correspondence in 2 or one distance could lead to competitive inhibition of DA signaling.

As seen from Table 2, all three listed values of O, O, O distances in 6B are closely similar to those in DA. This indicates that 6B can lead to competitive 3-point interaction similar to DA itself, causing agonistic influence. Also, two of the O, N, O distances in 8B, 2B, and 3B are closely similar to that in dopamine, while the third distance is distinctly shorter. As 2B can not penetrate BBB, competitive binding of 8B or 3B at the active site may lead to compression and thereby give a weaker interaction or distortion in the DA-receptor protein. Metabolites 7B and 4B had only one distance similar to that in dopamine and thus are expected to cause an inhibitory effect upon competitive binding with the DA-receptor unit. The hetero atom distances in metabolites 1B and 5B are grossly dissimilar to those in dopamine and thus these metabolites are thought to be incapable of giving any competitive binding at the receptor site. However, all metabolites can also exert allosteric π-interaction with receptor protein domains rich in amino acid residues with aromatic side chains, viz., phenylalanine, tyrosine, tryptophan, and histidine.

4.4. Comparative assessment

Consequent to discussions as above, the relative BBB permeability of the metabolites and suitability of N/O distance therein for receptor binding in the brain are summarized in Table 3. It could be seen that metabolites 3B, 4B, 6B and 8B are likely to exhibit superior BBB penetrability than ADTN, dihydrexidine and DPAT. Also that 6B can give efficient, competitive binding with DA receptors. Thus, it is inferred that parent dyes, i.e., Amaranth dye are likely to exert the strongest ADHD effect.

Table 2. Interatomic distances in dopamine (DA), selected azo dye metabolites and DA agonist

Compound	Hetero atoms	a	b	c
DA	N, O, O	**8.02**	**7.45**	**2.82**
1B	N, O	5.70		
	O, O, O	**8.22**	9.03	2.31
2B	O, N, O	**8.02**	6.35	**2.99**
	O, O, N	**8.02**	9.03	**3.03**
3B	O, N, O	**7.84**	6.58	**2.79**
4B	N, O, O	5.64	4.87	**2.87**
5B	N, O	5.70		
6B	O, N, O	**7.84**	6.58	**2.78**
	O, O, O	**7.84**	**7.28**	**2.80**
7B	N, O, O	5.67	4.89	**2.82**
8B	O, O, O	**7.85**	5.24	4.84
	N, O, O	**7.85**	6.54	**2.85**
ADTN	N, O, O	**7.95**	6.57	**2.80**
Dihydrexidine	N, O, O	**7.85**	**7.29**	**2.81**
8-OH-DPAT	N, O	**7.98**		

Table 3. Comparison of BBB penetrability and ligand Binding abilities of hydroxylated amine metabolites and dopamine agonists

Molecule	MWt	cLogP	TPSA	DiffCoef	HBDH	N/O/O Distances		
						a	b	c
1B	+	+	++	+	+	- - -		
2B	+	- -	- -	+	+	+++	+	++
3B	+	+++	+++	+	+	+++	+	+++
4B	+	+++	+++	+	+	- - -	- - -	+++
5B	+	+++	+	+	+	- - -		
6B	+	+++	+++	+	+	+++	+++	+++
7B	+	+	+	+	+	- - -	- - -	+++
8B	+	+++	+ +	+	+	+++	++	+++
ADTN	+	+	+++	+	+	+++	+	+++
Dihydrexidine	+	+++	+	+	+	++	++	+++
8-OH-DPAT	+	+	- - -	+	+	+++		

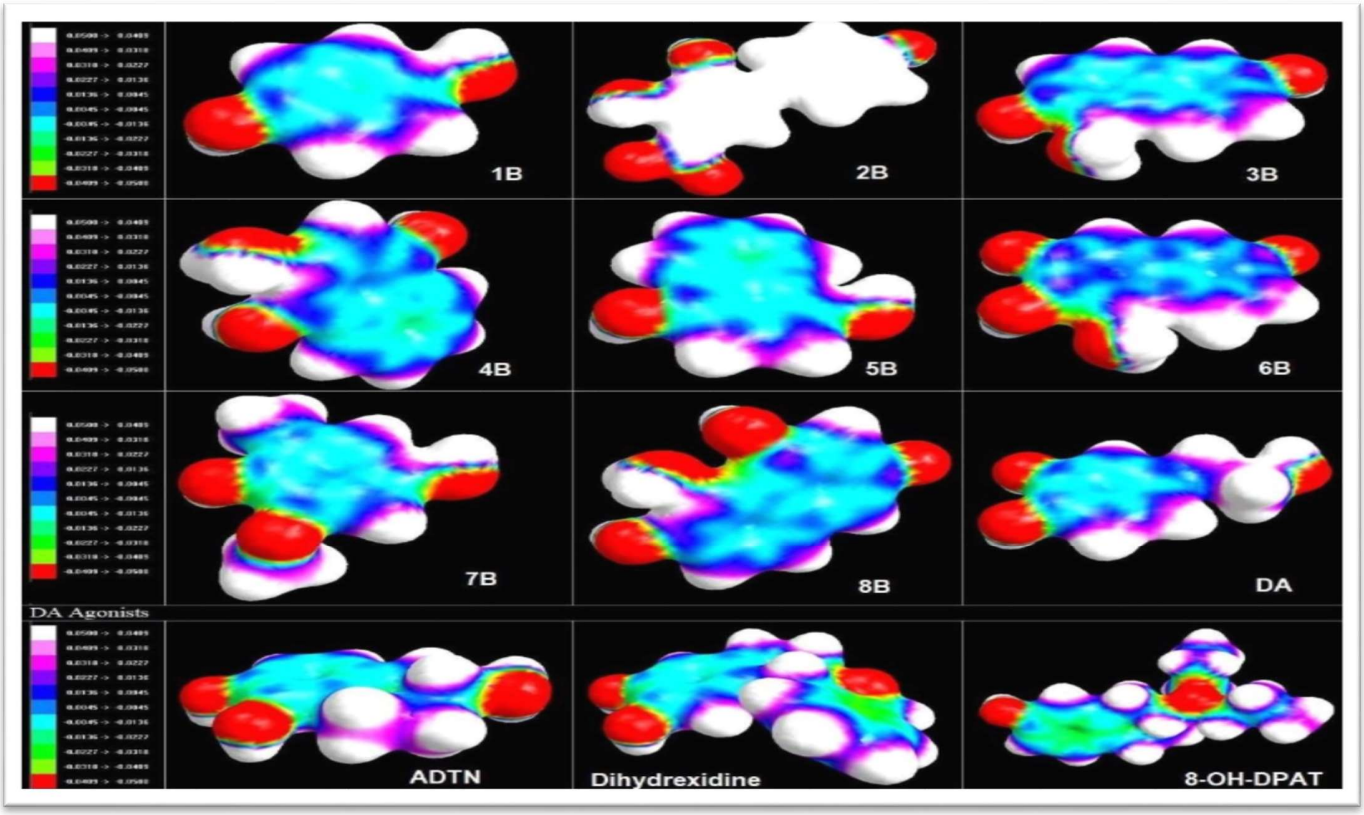

Figure 4. Geometries and Electrostatic Potential (ESP) distribution in aryl amino phenols, dopamine, and dopamine agonists

Tartrazine dye that produces metabolites 1B and 2B is least likely to cause ADHD, due to 1B's inability to interact with DA receptor units and 2B's inability to penetrate the BBB. Dye Sunset Yellow yields metabolites 1B and 3B, of which the latter possess good BBB penetrability and matched a and c distances, while compressing distance b. Competitive binding of 3B is likely to cause weaker DA triggering as compared to that of 6 B. Out of the two metabolites of Azorubine, i.e., 4B and 5B, the former has greater BBB penetrability and only a favorable distance c thus it is likely to compete with DA for receptor binding, causing an inhibitory effect. While 5B has poor BBB penetrability and an unfavorable N/O distance, and is expected to have no effect. Thus effect of Azorubine dye metabolite could lead to mild suppression of DA activity. Allura red produces 3B and 7B metabolites, out of which the former has good BBB penetrability and competitive DA-receptor binding ability, but the latter possesses poor penetrability and only one favorable N/O distance. :The effects of both metabolites are expected to cause competitive inhibition of DA activity. Dye Ponceu 4R yields 5B and 8B, of which 8B exhibits moderate BBB penetrability and competitive binding interaction similar to ADTN and dihydrexidine. Thus, it may lead to a stronger ADHD effect, similar to Sunset Yellow and Allura Red.

5. Conclusion

Considering BBB penetrability and competitive DA-receptor binding abilities of the azodyes' metabolites, it could be concluded that metabolites of Amaranth dye are likely to cause the strongest ADHD effect, followed by PonceauPonceau 4R, Allura Red, and Sunset Yellow. Dyes Azorubine and Tartrazine could cause milder ADHD effects. Generalization presupposes that reductive cleavage and hydroxylation of dissociation products occur to a comparable extent for all dyes.

Funding

No external funding was received for this research.

Authorship contributions

Mutual discussions between authors Katyayani Verma (KV) and Rajendra Prasad (RP) led to the conceptualization of the research. RP contributed to computational work. Both authors contributed to the literature review, data analysis, and interpretation as well as writing and editing of the original draft and its subsequent revisions.

Conflict of interest

The authors declare that they have no known competing financial interests or personal relationships that could have appeared to influence the work reported in this paper.

Data availability

Data will be made available on request.

Acknowledgment

The researchers (authors) of this paper dedicated their time, effort, and intellectual thinking to do this research voluntarily as part of intellectual inquiry, community education, and reducing potential risks to safeguard human health, particularly that of children.

References

1. Rambler RM, Rinehart E, Boehmler W, Gait P, Moore J, Schlenker M, et al. A review of the association of blue food coloring with attention deficit hyperactivity disorder symptoms in children. Cureus. 2022; 14(9): e29241.
2. Kirkland AE, Langan MT, Holton KF. Artificial food coloring affects EEG power and ADHD symptoms in college students with ADHD: a pilot study. Nutr Neurosci. 2022; 25: 159 – 168.
3. Boyle CA, Boulet S, Schieve LA, Cohen RA, Blumberg SJ, Yeargin-Allsopp M, et al. Trends in the prevalence of developmental disabilities in US children, 1997-2008. Pediatrics. 2011; 127: 1034 – 1042.
4. Weiss B. Synthetic food colors and neurobehavioral hazards: the view from environmental health research. Environ Health Persp. 2012; 120: 1.
5. Warner JO. Artificial food additives: hazardous to long-term health. Arch Dis Child. 2024; doi: 10.1136/archdischild-2023-326565 – 5.
6. Amchova P, Kotolova H, Ruda-Kucerova J. Health safety issues of synthetic food colorants. Regul Toxicol Pharmacol. 2015; 73: 914 – 922.
7. Moradi-Khatoonabadi Z, Amirpour M, Akbari Azam M. Synthetic food colours in saffron solutions, saffron rice and saffron chicken from restaurants in Tehran, Iran. Food Addit Contam B. 2015; 8: 12 – 17.
8. Anfossi L, Baggianim C, Giovannoli C, Giraudi G. Development of enzyme-linked immunosorbent assays for Sudan dyes in chilli powder, ketchup and egg yolk. Food Addit Contam A. 2009; 26: 800 – 807.

9. Curatolo P, D'Agati E, Moavero R. The Neurobiological Basis of ADHD. Ital J Pediat. 2010; 36: 79 – 85.
10. Sinn N. Nutritional and dietary influences on attention deficit hyperactivity disorder. Nutr Rev. 2008; 66: 558 – 568.
11. McCann D, Barrett A, Cooper A, Crumpler D, Dalen L, Grimshaw K, et al. Food additives and hyperactive behaviour in 3-year-old and 8/9-year-old children in the community: a randomised, double-blinded, placebo-controlled trial. Lancet. 2007; 370: 1560 – 1567.
12. Stevens LJ, Kuczek T, Burgess JR, Stochelski MA, Arnold LE, Galland L. Mechanisms of behavioral, atopic, and other reactions to artificial food colors in children. Nutr Rev. 2013; 71: 268 – 281.
13. Salamy J, Shucard D, Alexander H, Peterson D, Braud L. Physiological Changes in Hyperactive Children Following the Ingestion of Food Additives. Int J Neurosci. 1982; 16: 241 – 246.
14. Pelsser LM, Buitelaar JK, Savelkoul HF. ADHD as a (non) allergic hypersensitivity disorder: A hypothesis. Pediatr Allergy Immunol. 2009; 20: 107 – 112.
15. Walker R. The metabolism of Azo compounds: A review of the literature. Food Cosmet Toxicol. 1970; 8: 659 – 676.
16. Feng J, Cerniglia CE, Chen H. Toxicological significance of azo dye metabolism by human intestinal microbiota. Front Biosci (Elite Ed.). 2012; 4: 568 – 586.
17. Chung KT, Stevens SE, Cerniglia CE. The reduction of Azo dyes by the intestinal microflora. Crit Rev Microbiol. 1992; 18: 175 – 190.
18. Galli CL, Marinovich M, Costa LG. Absorption, distribution and excretion of 14C-carmoisine in mice after oral and intravenous administration. Food Cosmet Toxicol. 1981; 19: 413 – 418.
19. Lindstrom HV, Hansen WH, Nelson AA, Fitzhugh OG. The metabolism of FD&C Red No. 1. II. The fate of 2,5-para-xylidine and 2,6-meta-xylidine in rats and observations on the toxicity of xylidine isomers. J Pharmacol Exp Therap. 1963; 142: 257 – 264.
20. Zhao Z, Nelson AR, Betsholtz C, Zlokovic BV. Establishment and dysfunction of the blood-brain barrier. Cell. 2015; 163: 1064 – 1078.
21. Rishton GM, LaBonte K, Williams AJ, Kassam K, Kolovanov E. Computational approaches to the prediction of blood-brain barrier permeability: A comparative analysis of central nervous system drugs versus secretase inhibitors for Alzheimer's disease. Curr Opin Drug Discov Develop. 2006; 9: 303 – 313.
22. Pajouhesh H, Lenz GR. Medicinal Chemical Properties of Successful Central Nervous System Drugs. NeuroRx. 2005; 2: 541 – 553.
23. Volkow ND, Wang GJ, Newcorn JH, Kollins SH, Wigal TL, Telang F, et al. Motivation deficit in ADHD is associated with dysfunction of the dopamine reward pathway. Mol Psych. 2011; 16: 1147 – 1154.
24. Volkow ND, Wang G-J, Kollins SH, Wigal TL, Newcorn JH, Telang F, et al. Evaluating the dopamine reward pathway in ADHD. Clinical implications. J Am Med Assoc. 2009; 302: 1084 – 1091.
25. Luna RA, Foster JA. Gut brain axis: diet microbiota interactions and implications for modulation of anxiety and depression. Curr Opin Biotechnol. 2015; 32: 35 – 41.
26. Thompson MA. ArgusLab 4.0. Planaria Software LLC, Seattle, WA. 2018. Available at http://www.arguslab.com/arguslab.com/ArgusLab.html/ Accessed January 10, 2018.
27. Dewar MJS, Zoebisch EG, Healy EF, Stewart JJP. The development and use of quantum mechanical molecular models. 76. AM1: A new general-purpose quantum mechanical molecular model. J Americ Chem Soc. 1985; 107: 3902 – 3909.
28. SimulationsPlus. MedChem Designer chemical structure drawing and property prediction. 2018. Available at

https://www.simulations-plus.com/software/medchem-designer/ Accessed August 16, 2018.

29. OSIRIS Property Explorer. 2019. Available at https://www.organic-chemistry.org/prog/peo/ Accessed January 21, 2019.
30. Goodwin JT, Conradi RA, Ho NFH, Burton PS. Physicochemical determinants of passive membrane permeability: role of solute hydrogen-bonding potential and volume. J Med Chem. 2001; 44: 3721 – 3729.
31. Sgritta M, Dooling SW, Buffington SA, Momin EN, Francis MB, Britton RA, et al. Mechanisms Underlying Microbial-Mediated Changes in Social Behavior in Mouse Models of Autism Spectrum Disorder. Neuron. 2019; 101: 246 – 259.
32. Schmidt TSB, Raes J, Bork P. The Human Gut Microbiome: From Association to Modulation. Cell. 2018; 172: 1198 – 1215.
33. Kriss M, Hazleton KZ, Nusbacher NM, Martin CG, Lozupone CA. Low diversity gut microbiota dysbiosis: Drivers, functional implications and recovery. Curr Opin Microbiol. 2018; 44: 34 – 40.